TALYS: A tool to go from theoretical modeling of nuclear reactions to evaluations.

S. Hilaire

CEA, DAM, DIF
F-91297 Arpajon, France

Abstract

The TALYS code development started in 1998 in order to exploit the new computers which were appearing at that time and to have a tool which would be easier to improve than the other available codes. Since then, it has incorporated many new models that have appeared and has been made compatible with other codes in order to establish a link between nuclear reaction modelling and nuclear data evaluations.

A nuclear reaction calculation involves several models linked together, whose quality and validity are more or less well established. The oldest models, used since the beginning of nuclear reaction studies are the optical model and the compound nucleus model. These models correspond to two extreme situations in terms of the time required for a nuclear reaction to take place. The optical model corresponds to the fastest interaction process between a projectile and a target, while the compound nucleus process is the longest one, corresponding to the situation where the projectile has been absorbed in the target and has shared its energy with the target constituents. Between these two extreme cases, stands the pre-equilibrium process whose role becomes significant only beyond an energy threshold.

The practical implementation of these models requires other ingredients, which are either provided by complementary models such as those for level densities or for fission processes or directly taken from experimental databases such as discrete level properties or nuclear masses, eventually completed by theoretical predictions when necessary.

We will review all these models implemented in the TALYS code and will illustrate, with several examples, the large possibilities offered by this code, either to perform in depth nuclear reaction analysis or to produce large nuclear reactions' databases.

1. Introduction

Nuclear reaction models, beyond the fundamental quest for understanding processes taking place when a nuclear reaction occurs, are necessary to produce nuclear data for various applications. Depending on the targeted goal, the accuracy of the predictions as well as the type of data predicted might be very different. For nuclear reactors for instance, the accuracy is a clearly a key issue for specific nuclei and specific types of data. At the other extreme, one finds nuclear astrophysics for which the accuracy is less crucial than the ability of the model to produce data for all possible interacting systems. Even for the most important nuclei, for which many measurements have been performed, the need for better nuclear reaction models is still relevant since one still have to deal with processes for which data are not available or not precise enough. Within this context, nuclear reaction models have to be as robust and

predictive as possible. This is why during the last forty years at least, many nuclear reaction codes have been developed and used to answer the question: “what happens when a projectile hits a target nucleus?”.

It is clear that the answer to this question depends on the nature of the projectile, on the target and on the projectile energy. In what follows, we restrict ourselves to the case where a light projectiles (gamma, neutron, protons... up to ^{4}He) interacts with a target nucleus heavy enough (typically with a mass A>10) with an incident energy between 1 keV and 200 MeV, a framework enabling the implementations of the so-called “statistical models”. Within this framework, several models come into play. We will first describe in Section 2, general features observed when a nuclear reaction occurs at energies below 200 MeV, features that have motivated the introduction of several reaction models that will be discussed with more details in Section 3. In Section 4, we will focus on specific ingredients required by the reaction models as those related to fission for instance. Finally, Section 5 will be devoted to few practical illustrations of the possibilities offered by the TALYS code implementing these models.

2. General features about nuclear reactions

For incident projectiles with energy between a few keV and 200 MeV impinging on a target nucleus, the typical outgoing particle spectrum displays three main domains as illustrated in Fig.1. Two extreme regimes can be distinguished. For high outgoing energies, and forward angles, discrete peaks are observed and dominate the outgoing spectrum. Such processes correspond to fast interactions, also called “direct interactions”, which take place in a timescale comparable to the time the projectile takes to cross the nucleus. For low outgoing

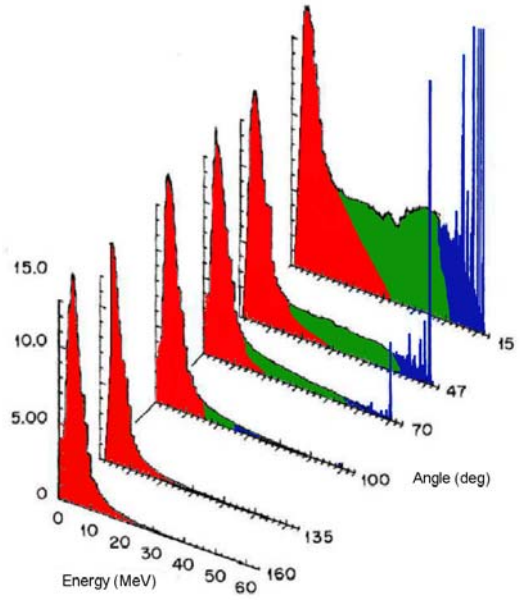

Figure 1: Outgoing proton spectrum observed for an incident proton on a ^{56}Fe target with 62 MeV of kinetic energy. Colors are used to distinguish the three regions corresponding to the direct reactions described by the optical model (blue), the pre-equilibrium model (green) and the compound nucleus model (red).

energies, a typical evaporation spectrum is observed. In this case, it is usually assumed that the projectile has been absorbed in the target with which it has shared all its energy to form a

compound system. This process, described by the so-called "compound nucleus model", assumes to the first order of approximation, that the formation and decay of the compound nucleus are independent processes. This assumption explains that the emission spectrum looks very similar (maxwellian shape) whatever the angle of emission is: the compound nucleus has lost memory of the way it has been created! This feature is characterized by angular distribution of emitted particle symmetric around 90°. Between these two extreme situations, one finds, if the projectile energy is high enough, an intermediate process whose frontiers are less well defined: the so-called pre-equilibrium process. This last process has been historically less studied than the two others (mainly because contrary to the two previous ones, it can be neglected for low incident energies) and therefore, the formalism which is employed to describe it is still subject to important debates and still offers room for significant improvements.

To these three types of processes, correspond in practice three types of models which are linked together, as illustrated in Fig.2, in order to produce many different types of nuclear data:the "optical model", the "pre-equilibrium model" and the "compound nucleus model".

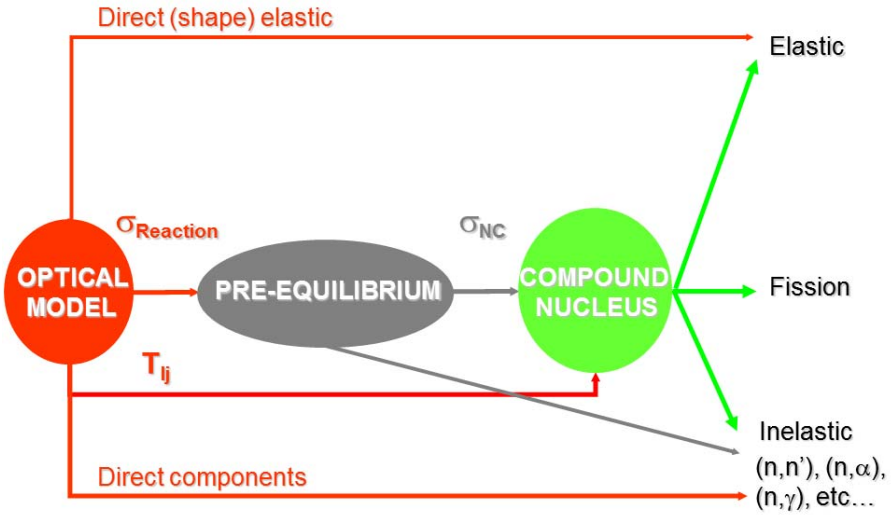

Figure 2: Sequence of nuclear models required to describe a nuclear reaction

All these models need to be implemented in a nuclear reaction code aiming at producing useful information. As can be observed, the optical model and the pre-equilibrium model both yield an output (elastic, fission or inelastic data) and also provides another model with an input ($\sigma_{Reaction}$, T_{lj} or σ_{NC}). The sole model only providing an output is the compound nucleus model.

3. Nuclear models for nuclear reactions

Before detailing the three nuclear models whose qualitative features have been discussed above in sections **3.b**,**3.c** and **3.d**, we first focus on nuclear structure data related to the target nucleus and the projectile that are mandatory to described a nuclear reaction.

a. Basic nuclear structure information

The most fundamental data required before even speaking of a nuclear reaction is the mass of the various nuclei that can appear during a decay process. This knowledge is necessary to determine reaction thresholds and to compute the kinematic relations enabling

laboratory to center of mass frame transformations. Other quantities such as nucleus levels' excitation energies, spins and parities are also welcome, if not necessary, and govern, as we will see later, various features of nuclear processes such as angular distribution or decay selection rules. Another feature also interesting though not mandatory is the deformed or spherical nature of the target. This information is particularly useful to adopt the proper treatment of the optical model as will be discussed in section **3.b**. Experimental nuclear masses are available today for nearly 2400 nuclei [Audi2012]. This set constitutes the reference data that nuclear mass models try to reproduce at best. Many different mass models have been developed during the last decades and the most advanced ones are able today to reach a deviation (**r.m.s**) from experiment close to 500 keV [Sobi2014], a remarkable level of accuracy with respect to the mass of a nucleus of the order of a GeV. Generally speaking, the more the nuclear mass models are based on first principle physics, the higher the predictive power should be. This feature has only been recently demonstrated by looking at the predictive power of various mass models adjusted on the 2003 atomic mass evaluation [Audi2003] with respect to the recent update of 2012 [Audi2012]. This analysis [Sobi2014] has indeed shown that only one microscopic mass model provides a better **r.m.s** when new masses are included.

b. The optical model

The optical model potential (OMP) is very important for nuclear reaction modeling because it is the one which determines the reaction cross section σ_R that the pre-equilibrium and compound nucleus models are then going to spread in the different outgoing open channels. It also provides the direct (or shape) elastic σ_{SE} and total σ_T cross sections ($\sigma_T = \sigma_R + \sigma_{SE}$), as well as the elastic angular distributions.

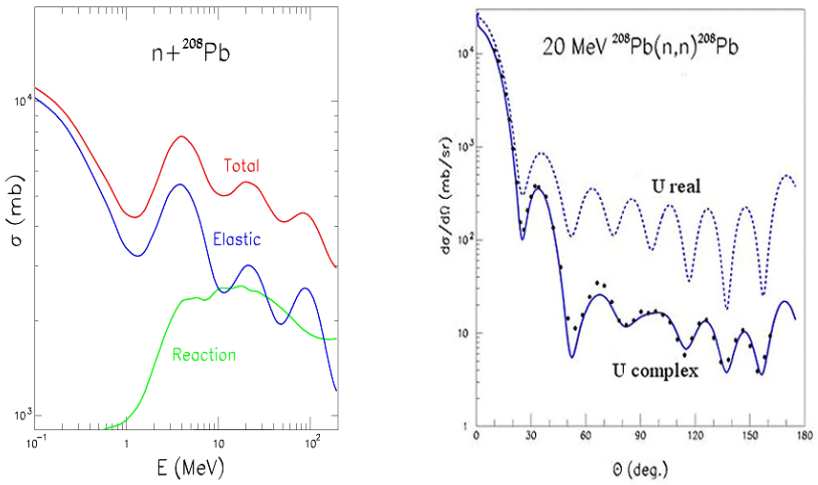

Figure 3: (left panel) Total, elastic and reaction cross sections and (right panel) elastic angular distribution obtained with a real or complex optical potential U.

The OMP describes the direct interaction of the projectile with the target nucleus as a whole thanks to a one body potential U introduced in the Schrödinger (or Dirac) equation.

$$\left(-\frac{\hbar^2}{2\mu}\nabla^2 + U - E\right)\Psi = 0$$

The wave function Ψ solution of this equation is determined using the partial wave expansion method, partial waves whose interferences explain the diffraction patterns observed on the right panel of Fig.3. As in optics, the potential can also (and even must) be complex, reading $U=V+iW$ and its imaginary part W then corresponds to a source term, which account for the

experimental evidence that part of the flux of incident projectile is lost in the elastic channel. *W* must then be negative to enable a proper description on experimental data. As can be observed in Fig.3, the effect of *W* is far from being negligible.

Historically, the OMP has been first determined postulating functional forms whose parameters have to be adjusted until a good agreement with data is obtained. This so-called "phenomenological approach" is still currently used in particular because of its ability to allow very accurate description of experimental data (total cross section with less than 1% accuracy). However, this approach depends very much on experimental data availability. Generally speaking, the OMP contains four components: a real Coulomb term and 3 imaginary nuclear components, namely, a volume, a surface and a spin orbit term. The three imaginary terms are moreover factorized into an energy dependent component and a radial component. For the radial part, one usually uses a Woods-Saxon expression similar to the matter distribution of the target nucleus $f(r,a,R)=-1./(1+\exp((r-R)/a)))$ for the volume term, and either a Gaussian or the derivative of a Wodds-Saxon function $=-d/dr\ f(r,a,R))$ for the surface term. Concerning the spin-orbit radial part, a Thomas form factor, $-1/r\ d/dr\ f(r,a,R))$, is usually chosen. The energy dependent parts have more or less complicated analytical forms depending on the energy range over which they are expected to be used or the mass region for which they are valid. A general feature however, is that for low incident energy the imaginary part of the potential is dominated by the surface term which smoothly vanishes while the volume part increases. This feature is related to the fact that the projectile only penetrates deeply in the target if its incident kinetic energy is high enough, otherwise it is mostly interacting at the surface of the target. Whatever the situation is, a phenomenological OMP always contains around 20 parameters that are fined tuned and enable to reproduce experimental data with high accuracy. Let us mention that thanks to experimental databases development (see [EXFOR] for instance) and computer power increase, systematic analysis of data have been made possible yielding global optical models usable over both a wide mass and energy range (see [Koni2003] for instance). It is also important to point out that additional constraints can be used thanks to dispersion relations linking real and imaginary parts of the potential therefore reducing the number of parameters to be adjusted [Mori2004].

An alternative to the pure phenomenological approach is the microscopic approach. Such approaches enable to determine the OMP without any a priori knowledge of any related experimental data. Therefore, they have the advantage of enabling predictions even for exotic nuclei far from the valley of stability which have not been measured and will probably remain, for many of them, out of reach from an experimental point of view. The disadvantage of such microscopic approaches is of course a lower accuracy, of the order of 5 to 10 % to be compared with the 1% accuracy obtained with a phenomenological OMP. Such a difference in quality is illustrated in Fig. 4.

The determination of a microscopic optical potential is possible performing a convolution of an information related to the target nucleus structure together with an effective interaction independent of the nucleus (see [Baug2001,Dupu2006] and references therein for details). The obtained potential is very sensitive to the quality of the structure description. One of the most employed approach is the so-called JLM approach [Baug2001] which is based on the nuclear matter densities or density matrix obtained from a mean field or beyond mean field approaches for instance [Hila2007,Dela2010,Dupu2010]. Such structure methods generally provide a nuclear structure description, which is hoped to be precise enough to guaranty that predictions far from the valley of stability should not be too far from the reality.

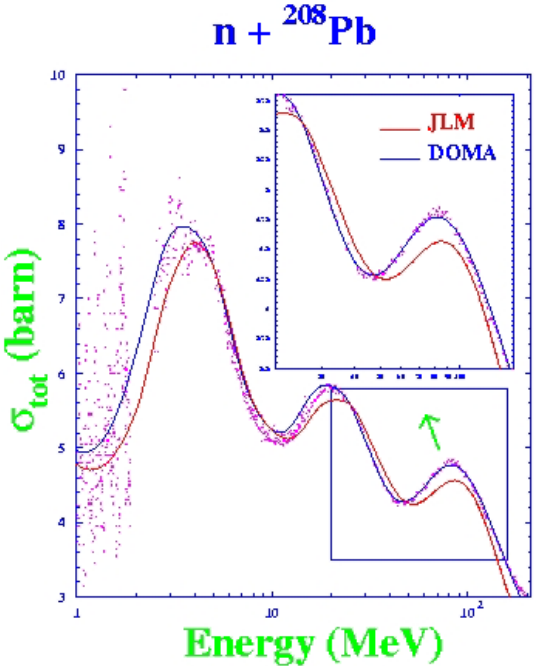

Figure 4: Comparison of the quality of the description of the total cross section for neutron induced reaction on ^{208}Pb obtained using a phenomenological dispersive OMP (blue) or a semi-microscopic OMP (red). Experimental data are reported with pink dots.

The choice between the two aforementioned approaches is guided by the goal one has in mind. Within the framework of nuclear data evaluation where accuracy is one of the key issues, availability of experimental data will make it preferable to use of a phenomenological OMP because of its fitting power. For more fundamental research or when there is a lack of data, the microscopic option will be preferred. Another important point to mention here concerns the possible deformation of the target nucleus which will also have an impact on the OMP treatment. Most of the nuclei are indeed deformed in their ground state and therefore exhibit rotational bands (excited levels) whose members are strongly coupled to the ground state. Such a coupling; when properly accounted for; yields on top of the shape elastic component a direct inelastic contribution (see Fig.2) which will be added to compound nucleus contributions to inelastic channels. Last but not least, coupling between the ground state and vibrational levels must also sometimes be accounted for, which further complicates the OMP design.

c. The pre-equilibrium model

Once the OMP has treated the various direct processes (elastic and inelastic), the remaining cross section, which correspond to all the processes which have not been explicitly accounted for is « feeding » the second model of Fig.2, the pre-equilibrium model. This reaction cross section reflects somehow the probability that the projectile be captured in the continuum of the target, therefore forming a « composite » system. At this stage, the system still remembers the way it was formed and is going to de-excite either by re-emitting a particle or by distributing step by step the incident projectile energy between one or several nucleons of the target. In the latter case, several particles and holes are going to be created sequentially, starting first with 2 particles and 1 hole and holding on towards more complex configurations as illustrated in Fig.5, to reach, after a sufficient time a situation corresponding to the compound nucleus approximation, where the projectile energy has been shared among all the constituents of the composite system. At each step of this process, the probability to emit a particle has to be accounted for.

As already written in Section 2, particles emitted during the pre-equilibrium process keep track of the incident projectile direction and are thus still forward peaked. However, emissions occurring after several steps look more and more symmetric around 90°, as well as, simultaneously, the emission energy is less and less close to the incident projectile energy.

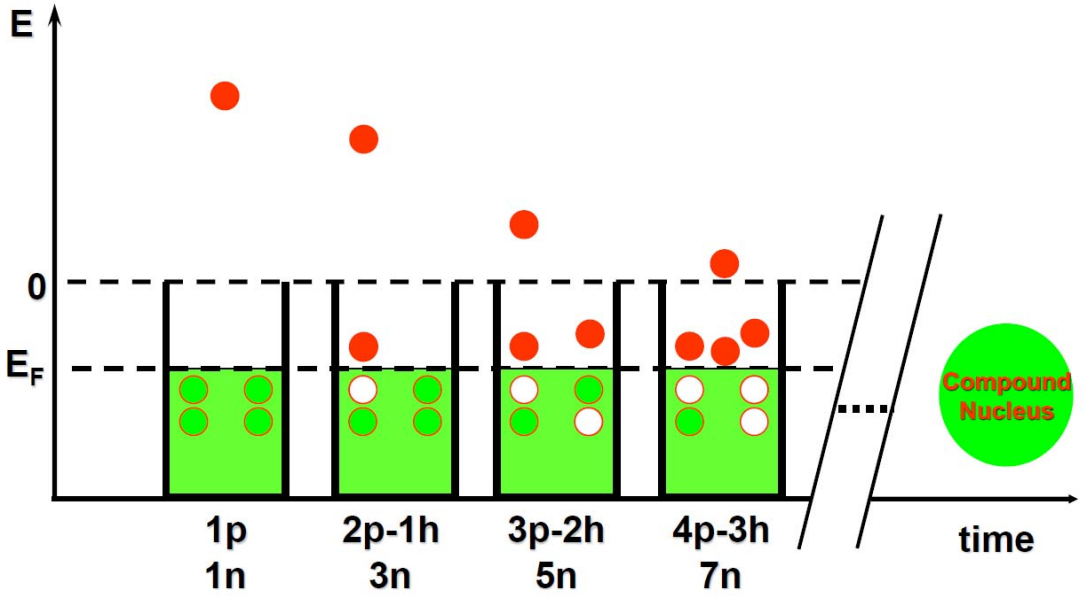

Figure 5: Schematic representation of the pre-equilibrium process. Within the exciton model framework, the number of exciton n=p+h is the sum of the number of particles p and holes h created to reach step by step a statistical situation in which the incident projectile energy will be shared among "all" the fermions constituting the composite system (projectile+target). In each step of this sequential process, there is a possibility to emit one of the unbound particles (i.e. those having a positive energy). After sufficient time, the system theoretically reaches an equilibrated compound nucleus.

Several pre-equilibrium models have been developed with more or less refinements. The first model, the so-called exciton model, introduced in the seventies, has been successively improved to account for more and more physical features either because the appearance of new experimental data evidenced a lack of predictive power or simply because initially missing though important features were sequentially introduced [Koni1998]. This semi-classical approach is by far the most often employed when one is interested in nuclear data applications. Quantum mechanical approaches have also been developed but they are clearly more complex and less flexible [Agas1975,Tamu1982,Fesh1980] and also provide results of similar quality as those obtained with the exciton model. However, recent experimental measurement seem to show that such quantum mechanical approaches are unavoidable if one aim at improving the models' predictive power (see Section 5).

An illustration of the impact of pre-equilibrium process is shown in Fig.6 in the case of the exciton model. As can be observed, without pre-equilibrium, excitation functions for multiple neutron emission (right panel) increase faster than when pre-equilibrium is accounted for. This stems from the fact that in the first situation, the amount of excitation energy given to the compound nucleus is higher than in the second case. Also, one observes that a pre-equilibrium component increases the high energy cross section and improves the agreement with experiment. In the left panel, the impact of the pre-equilibrium is also very clear. It produces more high energy outgoing neutron because of the possibility to emit a particle at each step of the process (see Fig. 5) towards statistical equilibrium.

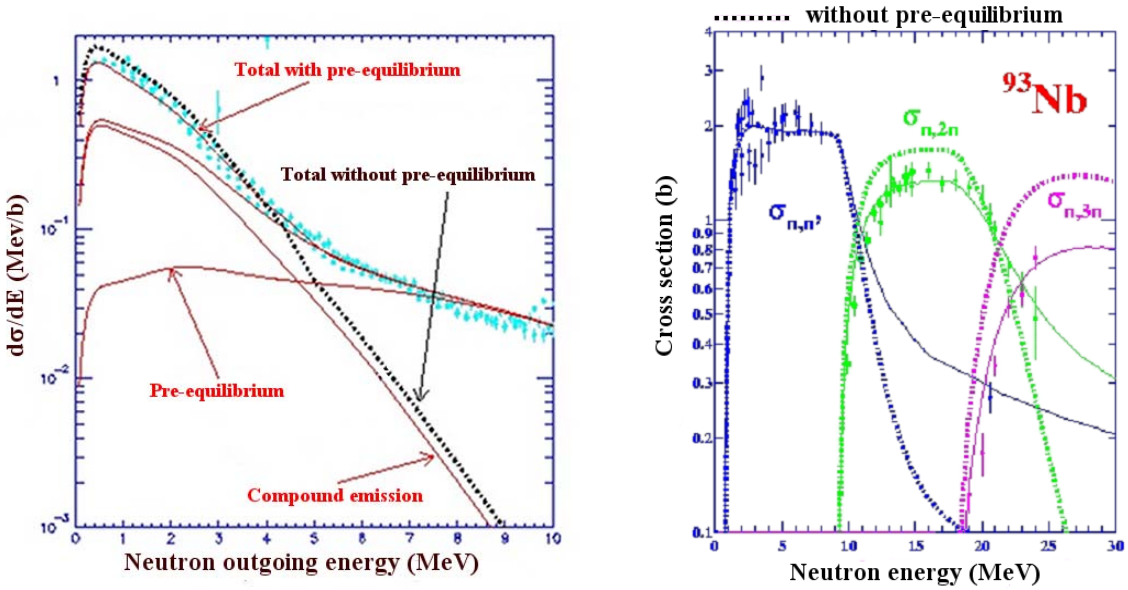

Figure 6 : Impact of the pre-equilibrium process on (left panel) outgoing particle spectrum and (right panel) excitation functions for neutron induced reaction on ^{93}Nb.

d. The compound nucleus model

Beyond the fact that optical and pre-equilibrium models contribute to the emission of particles, they are also those which determine the initial conditions of the last model of the chain shown in Fig.2: the compound nucleus (CN) model. Starting from such initial conditions, the CN model then uses the statistical hypothesis stating that the decay in a given outgoing channel depends on the ratio of the probability to decay in this specific channel with respect to all possible decay probabilities. This approximation, which consists in considering that the decay of the CN does not keep track of the CN formation (the Bohr hypothesis), is formally translated into the so-called Hauser-Feshbach [Haus1952] equation, reading

$$\sigma_{ab} = \sum_{J,\pi} \sigma_a^{NC}(E^*, J, \pi) \frac{\langle \Gamma_b(E^*, J, \pi) \rangle}{\sum_c \langle \Gamma_c(E^*, J, \pi) \rangle}$$

In this equation, the cross section σ_{ab} corresponding to the decay in channel b (particle type, energy, outgoing angular momentum) from the compound nucleus formed in the entrance channel a, is given by the product of the CN formation cross section σ_a^{NC} at a given energy, spin and parity *(E*, J, π)* by the probability to decay in channel b given all open channels c. The question therefore consists in estimating all possible average decay widths Γ_c. The Hauser-Feshbach approximation enables to write, to the first order approximation, that

$$\frac{\langle \Gamma_b(E^*, J, \pi) \rangle}{\sum_c \langle \Gamma_c(E^*, J, \pi) \rangle} = \frac{\langle T_b^{J\pi}(E^*) \rangle}{\sum_c \langle T_c^{J\pi}(E^*) \rangle} \quad ,$$

where the transmission coefficients $<T_c>$, which will be further discussed in Section 4, correspond to the decay probability in outgoing channel c (note that this expression becomes much more complicated when spin and parity conservation rules are explicitly written). Soon, it was realized that this first order approximation had to be corrected at low energy, or, more precisely when the number of competing channel is relatively low. In such situations, indeed, interferences, either constructive or destructive, occur between entrance and exit channels. These interferences are accounted for introducing the so-called width fluctuation correction

factor W_{ab}, which, generally enhances the elastic channel and accordingly decreases the other competing channels, but can also, in very particular situation, enhance the first inelastic channel [Kawa2013]. Several possible approaches have been developed and implemented to compute this correction factor [Hila2003] and find an optimum treatment.

e. Multiple Hauser-Feshbach decay

Untill now, we have only considered a single decay process, but in most situations, the residual nucleus reached after this first decay is still excited enough to further decay. The higher the incident projectile energy, the larger the number of possible decay will be. Therefore, in most cases, a multiple emission process has to be accounted for, until all residual nuclei are either in their ground state or in a metastable state considered as stable with respect to the nuclear reaction time. The principle governing these multiple decay processes are illustrated in Fig.7.

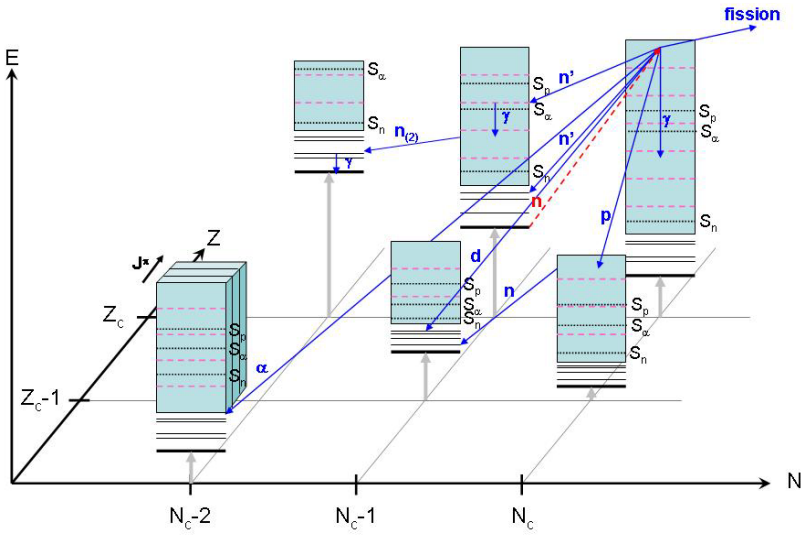

Figure 7: Illustration of multiple Hauser-Feshbach statistical emission

In this figure, each blue rectangle corresponds to a residual nucleus that will be populated during a multiple decay process. The compound system is the nucleus $[Z_c,N_c]$ obtained after the interaction of a neutron with the target nucleus $[Z_c,N_c\text{-}1]$ (red arrow). Each residual nucleus is characterized by a few discrete levels and several continuum energy bins, as well as particle separation energies (S_n, S_p, S_a, etc …) below which the corresponding particle emission is not possible. Starting from the initial state (end of the red arrow), all open decay channels (γ, n, p, d, t, ^{3}He, α) are going to be treated one by one to produce all corresponding residual nuclei either in a state from which only further γ-decay will be possible (state below all particle separation energies) or in a state where a second particle can be emitted. In the latter situation, the emission of a second particle will create another residual nucleus which in turn will decay in the various open channels. This sequential process discussed in terms of excitation energies constraining the various open channel is also constrained by parity and spin selection rules.

4. Nuclear reaction models ingredients

The models described in the previous section require specific ingredients depending on the outgoing channel under consideration. To be more precise, the OMP only provides transmission coefficient for outgoing particle decay to a well-defined level of the residual

nucleus. However, it does not enable to deal with the decay in the residual nucleus levels' continuum, with photon emission, and does not provide either any fission decay probability. These three situations require supplementary particular approximations that we now discuss.

a. Decay in a residual nucleus' continuum

When the projectile energy is large enough, the compound nucleus can decay by emitting a particle or a photon in the residual levels' continuum. This continuum has to be accounted for because it is well known that beyond a given excitation energy it is impossible to describe nuclear excited levels individually. In such cases, a nuclear level density (NLD) has to be introduced and the transmission coefficients entering the Hauser-Feshbach expression are given by the integral

$$\left\langle T_c^{J\pi}(E_c)\right\rangle = \int_{E_c-\Delta}^{E_c+\Delta} \rho(\varepsilon) T_c^{J\pi}(E_c) d\varepsilon$$

In this equation, E_c is the excitation energy remaining in the residual nucleus obtained after emitting a particle in a channel c and $\rho(\varepsilon)$ the residual nucleus level density in which we have omitted, for simplicity, the spin and parity labels which are implicitly included in the definition of the channel c according to the usual conservation laws of a binary nuclear reaction [Koni2008].

b. Photon emission

Whatever the projectile energy, gamma emission is always an open decay channel for which the residual nucleus turns out to be the compound system with a lower excitation energy, the difference being the energy of the emitted photon. To determine a gamma transmission coefficient $<T_\gamma>$, one assumes that photoabsorption and photoemission cross sections associated with a given decay type X (X=E or M for electric or magnetic transition) and a given multipolarity λ are related one with the other thanks to the same so-called γ-ray strength function. Experimentally, this strength function follows a Lorentzian shape, whose parameterization can be more or less sophisticated for E1 transitions [Capo2009], a few of them being illustrated in Fig.8. The magnitude of the strength function strongly depends, at

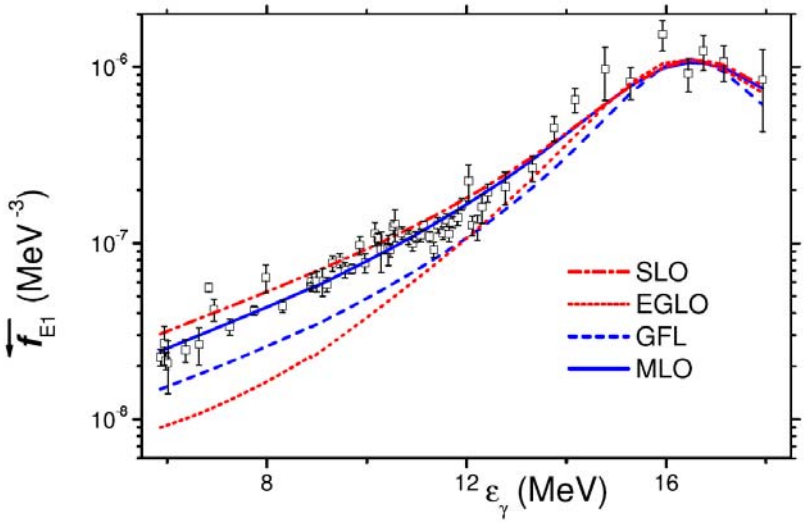

Figure 8: E1 γ-ray strength functions as function of the γ energy ε_γ with various phenomenological models compared with the experimental data of [Szef1983].

least close to the valley of stability, on both the type (E or M) and multipolarity of the emitted photon. Typically, E1 transitions are one to two orders of magnitude larger than M1, and more globally, an increase in multipolarity by one unit decrease by three orders of magnitude the corresponding strength. In sum, in most cases, E1 and M1 transitions are sufficient to obtain a good description of capture cross sections.
A specific feature of the capture process is due to the fact that the gamma decay occurs from the continuum of the compound nucleus to a very large number of levels, therefore requiring the use of a nuclear level density to be modelled, and, on top of that requires the knowledge of the strength for outgoing photon energies generally in the tail of the Lorentzian, quite far from the region where the experimental data which justify the use of the Lorentzian shape have been obtained. One has then two sources of uncertainty (level density and g-ray strength) which are combined to produce a total gamma ray transmission coefficient (or gamma ray width). For this reason, the theoretical gamma ray width is often quite different from the measured one, and a renormalization factor is introduced in the gamma-ray strength to improve either the agreement with the measured gamma ray width or with the experimental capture cross section data.

c. Fission channels

Despite its fundamental role in nuclear applications as a fundamental source of energy, as well as the fact that it has been discovered several decades ago and intensively studied since then, fission remains the least well understood process in nuclear reactions modelling.

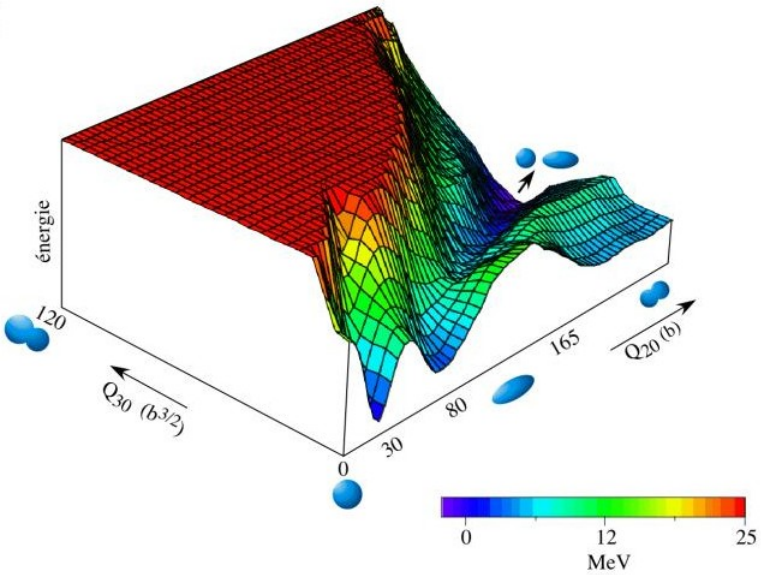

Figure 9: Potential energy landscape for ^{238}U as function of the two main deformation parameters (elongation, asymmetry) in which the colors indicated the energy difference between a given set of deformation parameters and the ground state energy of the fissioning system.

Qualitatively speaking, fission is modelled by a gradual transition of the nucleus from an initial compact shape to such an elongated shape that the nucleus breaks into two fragments (scarce events with more than two fragments also occur but are always neglected in nuclear reactions codes aiming at calculating cross sections). This evolution towards fission is governed by a potential energy landscape corresponding to nuclear shapes more or less probable depending on the excitation energy required to reach them. Such a potential energy landscape is illustrated in Fig.9. This landscape exhibits features such as valleys and peaks which help understanding the major characteristics of the fission process, and, in particular the fission fragments distributions observed experimentally. In Fig.9, for instance, the

asymmetric fission of ^{238}U is understood as the consequence of the fact that the exit point with non-zero asymmetry is more favorable energetically than the symmetric exit point, in particular because of the barriers (peaks) whose height is higher for Q_{30}=0. For cross section calculation, one does not use multidimensional approaches but instead an effective one dimensional approach which takes benefit from the general features illustrated in Fig.9 by introducing fission barriers which are then used to compute fission transmission coefficients.

Before detailing further the way fission transmission coefficients are calculated, the fission barrier concept already enables to distinguish between two well-known categories: the fissile and fertile nuclei. In the first case, a thermal incident neutron will induce fission since the binding energy of the neutron in the composite system is higher than the fission barrier height, while in the second case, non-negligible neutron energy is required (threshold) to induce a significant fission.

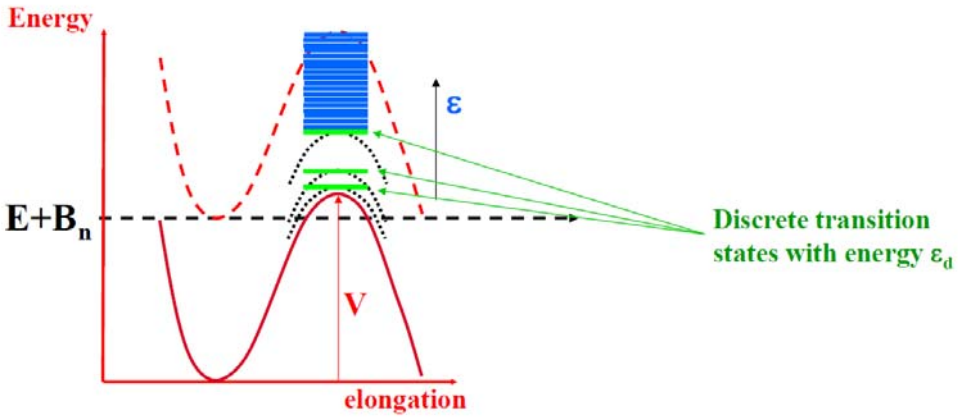

Figure 10: Illustration of a single humped fission barrier with discrete (green) and continuum (blue) transition states with energies corresponding to the definition of the fission transmission coefficient as introduced in the current section.

As previously mentioned, for nuclear cross section calculation, one introduces a one-dimensional fission barrier whose shape is moreover usually supposed to be parabolic and can be parameterized by its height V and its curvature $\hbar\omega$. The tunneling through such a potential barriers can then be analytically determined yielding the so-called Hill-Wheeler [Hill1953] formula,

$$T_{hw}(E) = \frac{1}{1+\exp\left(-2\pi\dfrac{E-V}{\hbar\omega}\right)}.$$

Given an initial compound nucleus state, fission occurs by tunneling through all accessible fission barriers (Bohr hypothesis) whose height are then that of the ground state V plus the energy of the so-called transition states ε located on top of the fission barriers (see Fig.10). Therefore, for a single barrier, the fission transmission coefficient is given by

$$T_f(E,J,\pi) = \sum_{d(J,\pi)} T_{hw}(E-\varepsilon_d) + \int_{E_c}^{E+B_n} \rho(\varepsilon,J,\pi)\,T_{hw}(E-\varepsilon)\,d\varepsilon\,,$$

equation in which ε corresponds to the transition states' energies. These transition states are discrete up to a given arbitrary threshold E_c, and, as for the compound nucleus at normal deformation, are then described by a nuclear level density $\rho(\varepsilon, J, \pi)$ beyond E_c.

In many cases, the potential energy surface (see Fig.9) does not only display a single humped fission barrier but rather two or even three. In the case of a double humped fission barrier, the fission transmission coefficient reads

$$T_2 = \frac{T_A T_B}{T_A + T_B},$$

where T_A and T_B are the fission transmission coefficients for each barrier. This expression can be easily generalized to more than two barriers (in practice, one never account for more than three barriers). For multiple humped fission barriers, one also account for the fact that there exist potential wells between the barriers in which quantum states can be located, usually called class II or class III states depending upon whether they are located between the first and second barrier or between the second and the third. If these class II/III states have a spin and parity corresponding to that of the compound nucleus from which fission occurs, they induced a resonance effect in the fission transmission coefficient as illustrated in Fig. 11 for which more or less refined treatments are possible [Koni2008,Sin2008].

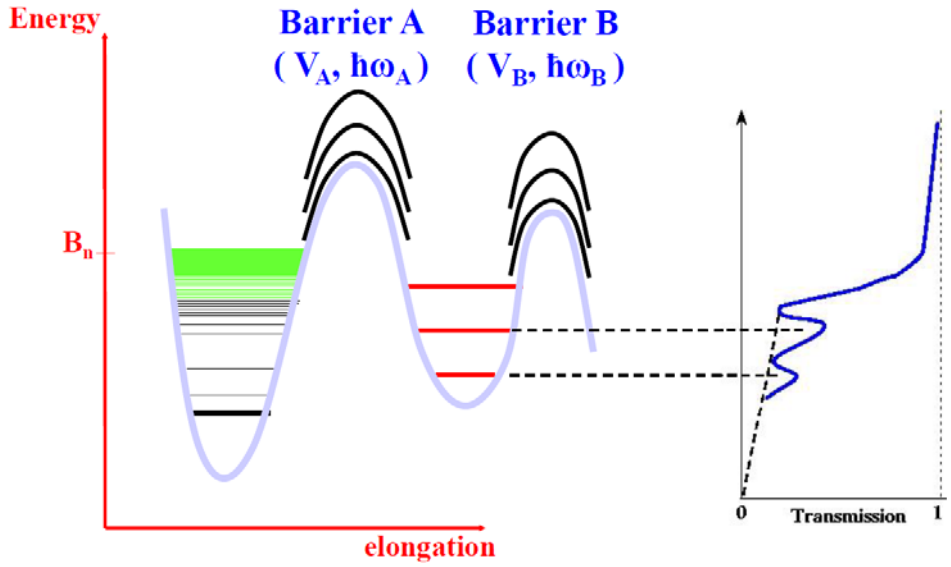

Figure 11: Illustration of a double humped fission barrier. The existence of class II induces resonant structures in the fission transmission coefficient.

d. Nuclear level densities

We have seen in the previous paragraphs the importance of the nuclear level densities as a mandatory quantity as soon as one cannot deal with discrete nuclear levels in the outgoing open channels. When considering neutron induced reactions, the need for nuclear level densities for outgoing particle emission only occurs if the incident energy enables the compound system to decay in a residual continuum bin. On the contrary, whatever the incident energy, the gamma emission always (or almost always) requires the introduction of nuclear level densities since even with low energy neutrons, the compound system decay from an excitation energy corresponding at least to the neutron binding energy, generally far above the last discrete level. Nuclear level densities have been widely studied for decades and we only summarize here their main qualitative features.

The need for nuclear level densities stems from two main observations, illustrated in Fig. 12, namely (i) the number of excited levels in the nucleus increases exponentially with increasing excitation energy (left panel) and (ii) cross sections for low energy neutrons display resonant structures interpreted as compound nucleus levels whose spacing can be of the order of a few

eV, therefore corresponding to a number of levels per MeV of the order of a million (right panel).

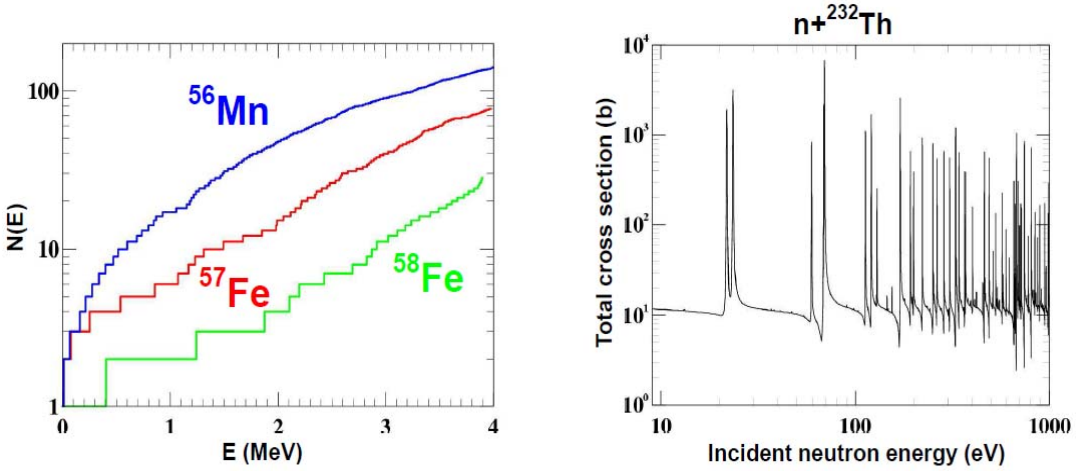

Figure 12: (Left) Cumulated number of discrete levels as function of the excitation energy. (Right) Total cross section for low energy neutron impinging on a ^{232}Th target.

For these two reasons, it is clear that one cannot treat each compound nucleus level individually. In practice, beyond a limited number of well identified discrete level (which can be only the ground state for exotic nuclei), a nuclear level density is therefore used whose analytical expression is usually the combination of the so-called "constant temperature" law,

$$\rho(E) = \exp\left((E - E_0)/T\right)$$

between the last discrete level and a matching energy of a few MeV above which the well-

$$\rho(U,J,P) = \frac{1}{2}\frac{\sqrt{\pi}}{12}\frac{\exp\left(\sqrt{2a\tilde{U}}\right)}{a^{1/4}\tilde{U}^{5/4}}\frac{2J+1}{2\sqrt{2\pi}\sigma^3}\exp\left[\frac{\left(J+1/2\right)^2}{2\sigma^2}\right],$$

known "Fermi Gas" law is adopted as function of the excitation energy U, the spin J and parity P of the levels under consideration. In the latter expression appears the level density parameter a, the spin-cut factor σ, whose expression generally reads

$$\sigma^2 = I\sqrt{\frac{\tilde{U}}{A}},$$

with I the nucleus' moment of inertia (or a fraction of it), and an effective energy $\tilde{U} = U - \Delta$, where Δ is an energy shift introduced to account for pairing effect whose consequence is a reduction of the number of levels in even-even nuclei with respect to odd-even ones and odd-odd nuclei (see Fig.12, left panel).

When the Fermi Gas expression is used to analyze s-wave experimental mean spacing D_0 (spacing of the resonances as observed in the right panel of Fig.12) at the neutron binding energy B_n, one observes that the level density parameter a displays strong deviations from a straight $A/8$ line (See Fig.13) which are correlated with the so-called energy shell δW (defined as the difference between experimental masses and those given by a simple liquid drop model). This correlation is often described using the following expression

$$a(N,Z,\hat{U}) = \tilde{a}(A)\left[1 + \delta W(N,Z)\frac{1-\exp(-\gamma\tilde{U})}{\tilde{U}}\right],$$

usually referred to as the Ignatyuk formula [Igna1975], which provides a practical expression to deal with the fact that the level density parameter increases with excitation energy for magic or nearly magic nuclei due to the strong shell effect which requires a significant energy to be washed out. The washing out of the shell effects is accounted for through the exponential function with the γ parameter and when shell effects are washed out, the level density parameter reaches its asymptotic value $\tilde{a}$ which is close to A/8 in the simplest expressions. In actual calculation, all parameters entering these expressions are fitted to reproduce experimental cross sections or taken from compilations such as the RIPL one [Capo2009].

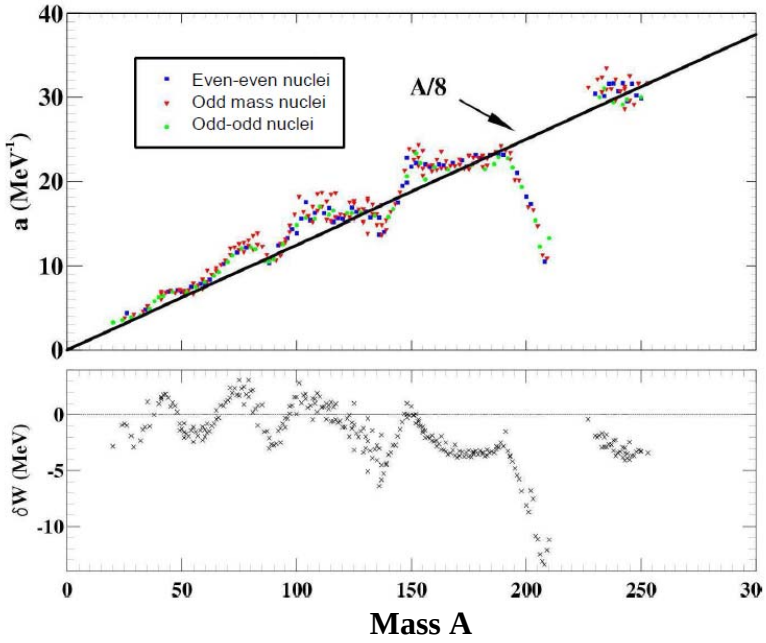

Figure 13: (Top) Level density parameter extracted from D_0 values at B_n (see text for details). (Bottom) Typical Shell corrections energy taken from the RIPL database [Capo2009].

If the above analytical expressions are those which are generally used, several alternatives are available based on more or less fundamental approaches. The so-called generalized superfluid model [Igna1985], for instance, accounts for more physical effect, such as collective effects, but it is at the price of more complications with an added value which does not yet makes a consensus for practical applications compared to the simplest forms. When dealing with exotic nuclei for which data are unavailable to adjust the parameters entering the analytical expressions, the only alternative, so far, is the combinatorial approach for which systematical calculations have been performed providing tables of nuclear level densities which have a quality comparable to global analytical models with the advantage of enabling one to deal with deviations from the statistical feature of the analytical approaches [Gori2008].

5. The TALYS code

All the models described in the previous section and the ingredients they require need to be implemented in a nuclear reaction code in order to provide one with nuclear reaction data, such as cross sections, angular distribution, double differential spectra, prompt neutron multiplicities, etc … in sum all nuclear data required to produce evaluated files required to feed macroscopic applications oriented research. Several nuclear reaction codes have been developed for more than 30 years (see for instance GNASH [Youn1992], ALICE [Blan1993], STAPRE [Uhl1976], EMPIRE [Herm2007]), and have more or less followed

the evolution of the available computer power. The TALYS code is among the latest one in this field and due to this late arrival, it has taken advantages of the modern computers which were emerging when its development started in the late 1990's and of some of their foreseen evolutions.

a. Generalities

TALYS [TALYS] is a nuclear reaction program whose development began in 1998 within a collaboration between NRG Petten and CEA, DAM, DIF. Its objective is to provide a complete and accurate simulation of nuclear reactions in the 1 keV-200 MeV energy range, through an optimal combination of reliable nuclear models, flexibility and user-friendliness. TALYS can be used both for the analysis of basic scientific experiments and to generate nuclear data for applications. The code has been developed following the mantra "First completeness then quality": This certainly should not suggest that toy models have been used to arrive at some quick and dirty results, but it rather means that to succeed in the quest for completeness, efforts have been equally divided among all nuclear reaction types. In other words, the choice has been made to avoid losing time to implement a perfect model for a nuclear reaction which accounts for only a few millibarns of the total reaction cross section, in order to preferentially enhance the quality of TALYS equally over the whole reaction range and always search for the largest shortcoming that remains after the last improvement.

As specific features of the TALYS code we mention:

- A clear (transparent and commented source program) and documented implementation (extensive manual) of many of the latest nuclear models for direct, compound, pre-equilibrium and fission reactions providing continuous and smooth description of reaction mechanisms over a wide energy range (1 keV - 200 MeV) and mass number range (12 <A< 339).
- Completely integrated optical model and coupled-channels calculations by the ECIS-06 code [Rayn1994] complemented by recent optical model parameterizations for many nuclei, both phenomenological (optionally including dispersion relations) and microscopic [Bauge2001].
- All possible outputs required to produce evaluated data for energies above the unresolved resonance range (URR) and eventually to generate parameters for the URR.
- Automatic reference to nuclear structure parameters as masses, discrete levels, resonances, level density parameters, deformation parameters, fission barrier and gamma-ray parameters, generally from the IAEA Reference Input Parameter Library [Capo2009] or from microscopic approaches with help of tabulated values.
- Option to start with an excitation energy distribution instead of a projectile-target combination, helpful for coupling TALYS with external codes (intranuclear cascade codes for instance) or fission fragment studies.
- Use of systematics if an adequate theory for a particular reaction mechanism is not yet available or implemented, or simply as a predictive alternative for more physical nuclear models.
- Astrophysical reaction rates using Maxwellian averaging.
- Input/output communication that is easy to use and understand, using several hundreds of keyword if a fit to experimental data is necessary or with a 4 line idiot proof input if default options are used.

The central message is that TALYs always provide a complete set of answers for a nuclear reaction (for all open channels and all associated cross sections, spectra and angular distributions) whose qualities depend on the current status of the nuclear reaction models (and

our ability to implement them) and of the ingredients they require. This robustness is regularly checked using external codes (not distributed) to perform drip line to drip line calculation with default options, to generate random input or to statistically analyze results smoothness and tendencies (see **Section 5.c**).

Last but not least, the code flexibility and robustness also enables automatic generation of nuclear data in ENDF-6 format [ENDF] (not included in the free release) as well as automatic optimization to experimental data and generation of covariance data (not included in the free release).

b. In depth nuclear reaction analysis

The large number of options of TALYS provides one with the possibility to fine tune model parameters or model ingredients to perform in depth nuclear reaction analysis. Several examples have been published in the literature of such a way of using the code and we only quote here two of them.

Impact of non-statistical level density

As summarized above, various level density models can be chosen while predicting the issue of a nuclear reaction. This kind of analysis, illustrated in Fig.14, has been performed in [Goko2006] to interpret the total photo-induced neutron decay of ^{181}Ta the partial one producing the first isomeric level ^{180}Ta^{m}. As can be observed in the left panel of Fig. 14,

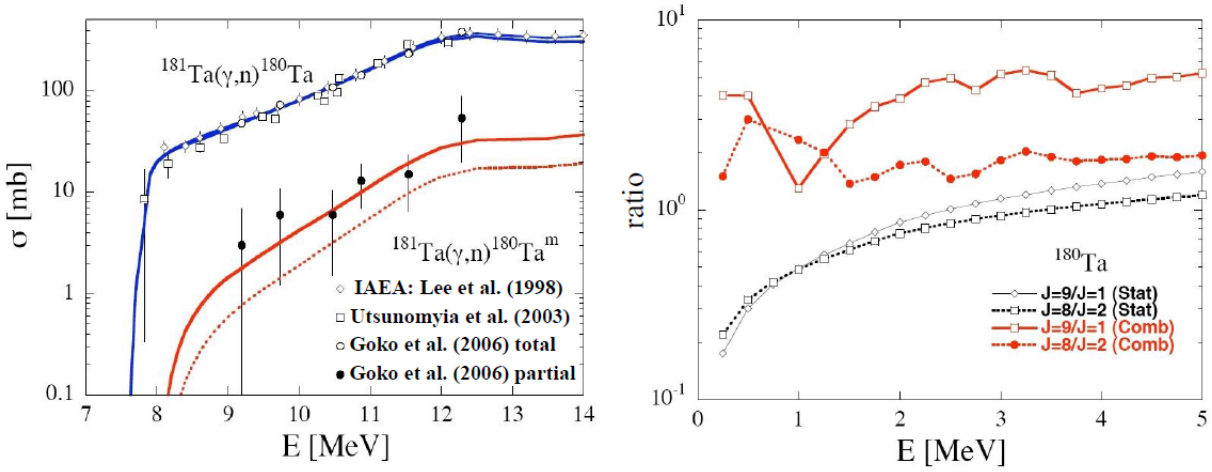

Figure 14: (Left) ^{181}Ta(γ,n) excitation function. (Right) Level density ratio for specific spins.

switching from a phenomenological level density model (dotted line) to a microscopic model (full line) significantly modifies the isomer production while almost not affecting the total (γ,n) excitation function. This particular case illustrates the importance of using a non-statistical spin-parity level density: indeed, as illustrated in the right panel of Fig. 14, the microscopically predicted level density of high spins is much higher than the phenomenological one, therefore increasing the decay probability to the first isomer ^{180}Ta^{m} and globally providing a natural explanation to the disagreement obtained with experimental data when using a phenomenological level density approach.

Coherent fission modelling

Fission is a complicated process whose modelling involves many parameters which have to be adjusted to reproduce at best experimental data. With increasing kinetic energy of the projectile inducing fission, several nuclei come into play. Above the neutron emission threshold for instance, multiple fission chances have to be described.
For a 10 MeV neutron incident on ^{238}U both ^{239}U (first chance fission) and ^{238}U (second

chance fission) fission barriers' parameters have to be fine-tuned and the higher the incident energy, the more the number of fissioning nuclei to consider. If this makes the fine tuning more complicated, it also provides a way to get more constraints than the single ^{238}U neutron induced fission cross section, provided one wants to coherently model the several fission chances.

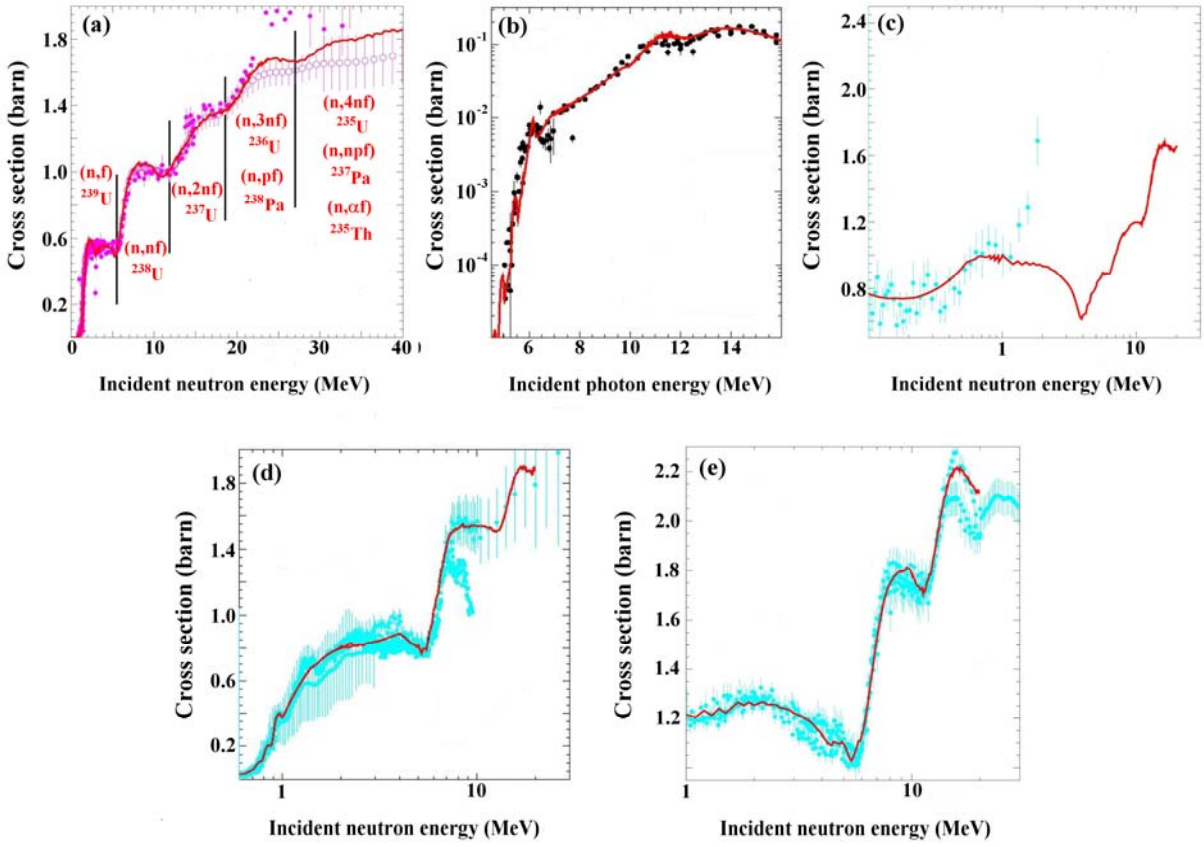

Figure 15: Illustrations of the coherent modelling of fission cross sections. (a) neutron induced fission cross section on ^{238}U. (b) photo-induced fission on ^{238}U. (c) neutron induced fission cross section on ^{237}U.(d) neutron induced fission cross section on ^{236}U.(e) neutron induced fission cross section on ^{235}U.In panel (a), the vertical lines indicate for which incident neutron energy new fissioning nuclei have to be accounted for (see text for more explanations).These fissioning systems are indicated in red as well as the emission process which makes it necessary to deal with them.

To be more precise, the fact that the fourth chance of ^{238}U fission is governed by the fission barriers of ^{236}U implies that the latter should also provide a good description of the first chance of ^{235}U since in both cases the nucleus which undergoes fission is the same. Another constraint can also be obtained by noticing that the fission barriers parameters enabling a proper description of photo-induced fission on ^{238}U should also provide a good second chance fission of neutron induced fission of ^{238}U. Therefore, a coherent modeling of fission means that the same set of input parameters should provide simultaneously the various fission chances of the various fissioning systems encountered within a given isotopic chain. An illustration of the results obtained using TALYS with such a modelling framework is given in Fig.15. If the price to pay by considering all these constraints is an important amount of work, the reward is a simultaneous description of a whole isotopic chain. In the case of ^{238}U induced fission indeed, fitting experimental fission cross section data up to 40 MeV requires to adjust the fission parameters for all Uranium isotopes between ^{239}U (first chance fission) and ^{235}U (fifth chance) as well as other fission chances due to the opening of proton emission and ^{4}He emission (see Fig.15).

c. Global nuclear reactions

The possibility to use TALYS without fine tuning parameters, i.e with the simplest possible input specifying the nature of the projectile, the target mass and number of protons and the projectile energy, provides one with the possibility of performing systematic calculation of cross sections. This feature enables to improve regularly the overall quality of default results provided by TALYS as well as to perform astrophysical relevant nuclear reaction calculations, for which one cannot afford to adjust model parameters because of the large number of nuclei for which reaction rates are required.

Astrophysical reaction rates

Beyond the fact that astrophysical rates are required for thousands of nuclei which makes it impossible to adjust model parameters, it is also preferable in such a framework to adopt models whose predictive power can be trusted. In this respect, several microscopic alternatives to the traditional analytic models used for fine tuning have been developed and stored as tabulated data in the TALYS database. They have then been tested by performing systematic comparison with experimental data, and, generally speaking, do not provide as such good results, or at least at the level required for practical applications. However, because of their microscopic grounds, it is believed that such approaches have good trends, and could be globally normalized to fit experimental data at best subsequently providing one with "trustable" extrapolations to regions where measurements are impossible.

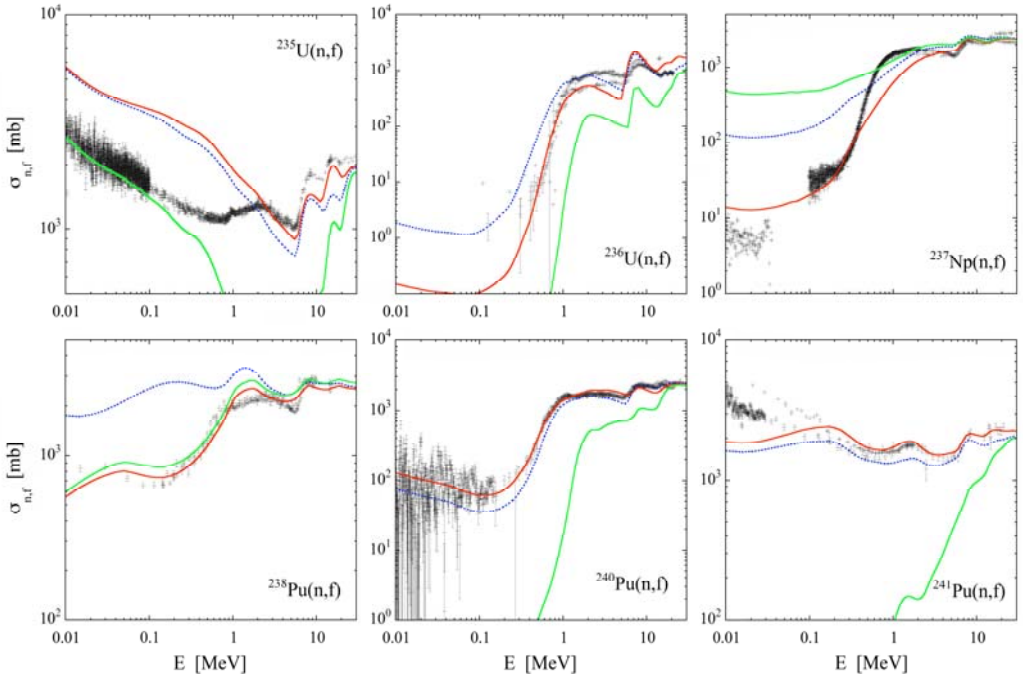

Figure 16: Illustrations of the global modelling of fission cross sections using microscopic inputs for fission paths as well as nuclear level densities. Default results are shown by the green curves. Red and blue curves show either individual or global normalized results (see text for details).

A typical example of such a methodology is illustrated in Fig. 16 in the case of the most complicated nuclear reaction process that is neutron induced fission. In this specific example, one has adopted microscopic options for all fission relevant nuclear level densities (both for ground state and on top of fission barriers) as well as for the fission barriers' shapes

themselves. Comparing the fission cross section with experiment does not yield by default very satisfactory agreement (green curves). The reason for this is the extreme sensitivity of fission cross sections to fission barriers' heights. Normalizing one by one the target fission barriers enables to improve significantly the agreement with experiment (red curves). However, such an approach only works for measured nuclei. In order to allow for a systematic use of microscopic barriers, the one by one normalizations have been averaged depending on the nucleus oddness and have thus reduced to 4 parameters (for odd-even, even-even, even-odd and odd-odd nuclei) which can be used for any nucleus (blue curves). Such a method enables to keep the global topology predicted by microscopic approaches for the fission barriers as function of elongation even if the heights are adjusted for a better agreement with measured cross sections.

Global analysis of cross sections

Another aspect of the possibility to use TALYS for global nuclear reaction calculation is the fact that it enables to check its robustness and the stability of the obtained results. Such an approach is used to suppress bugs or to improve the overall quality of the code.

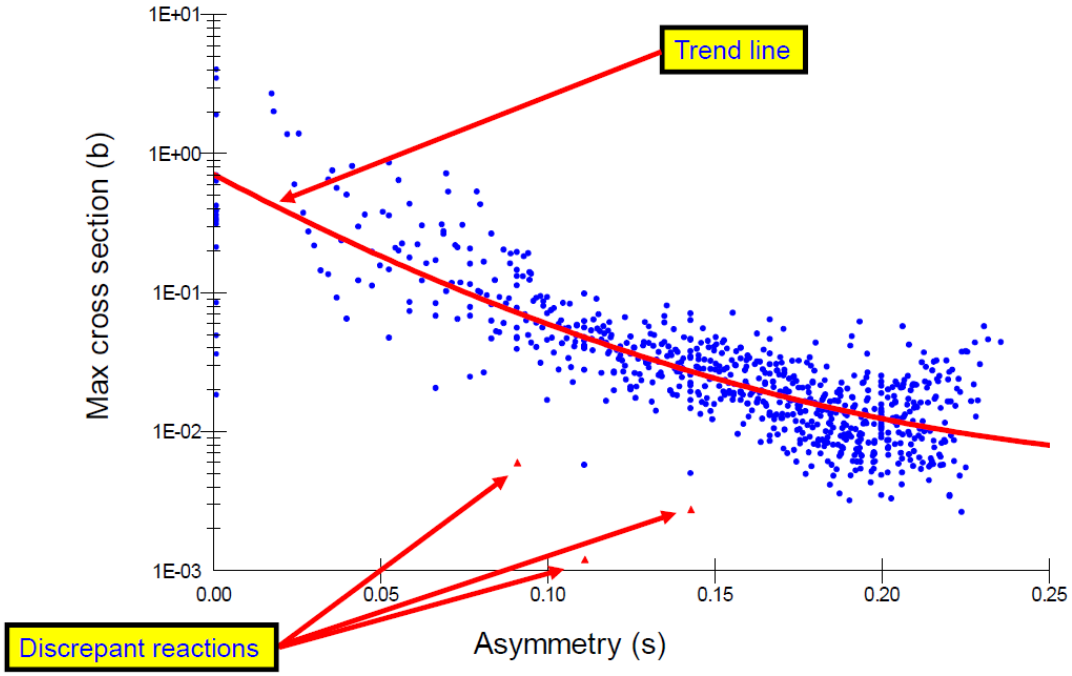

Figure 17: Maximum cross sections of all measured (n,p) reactions as function of the asymmetry s=(N-Z)/A.

It is illustrated in Fig. 17 for (n,p) reactions. The strong deviations from the trend line enable to analyze the sources of discrepancy. The same kind of analysis has been performed for other channels such as (n,2n), (n,γ) or (n,p) and are available online [TALYS]. The results for non-fissile nuclei are generally quite close to experiment. For fissile nuclei, again, a significant work generally remains to be done to obtain satisfactory results.

d. Covariances and Total Monte Carlo with TALYS

The large number of keywords of the TALYS code enables fine tuning to reproduce experimental data and provide high quality evaluations for applications. It also offers the possibility to sample around the "best" set within arbitrary ranges in order to study the results'

sensitivity to the various tunable parameters and compute covariance matrices which are important information to optimize the design of modern nuclear facilities.

Covariances with TALYS

Covariances are important data for design and safety of modern nuclear facilities. They provide the correlations between cross sections according to the model used to determine them. For instance, they enable to estimate what would be the impact on all open channel at various energies of a few percent increase of a specific cross section in a given energy range. By sampling a few relevant input parameters, thousands TALYS runs can be computed to determine dispersions around the central (or best) cross section value, as well as correlations between channels and energies.

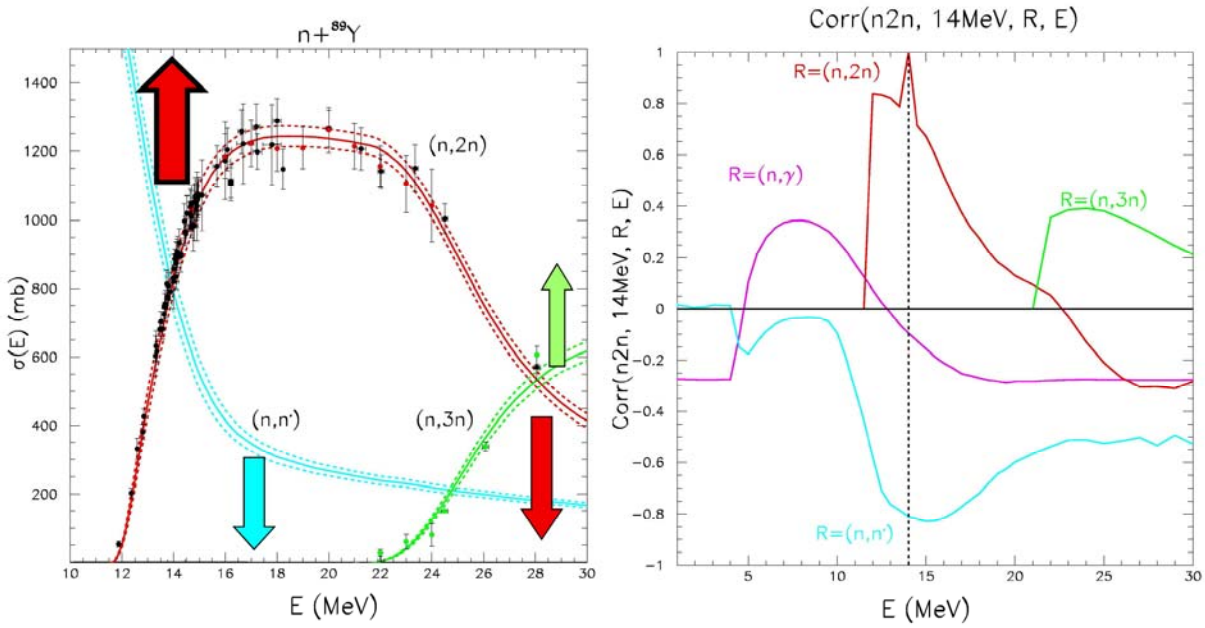

Figure 18: Illustrations of the correlations provided sampling the input parameters of TALYS for neutron induced reactions on ^{89}Y. (Left) Cross sections are shown by full lines, experimental data by dots, and dotted line correspond to the standard deviation of the various obtained results distribution. The arrow indicate how the cross section will be modified if one increases the (n,2n) around 14 MeV according to the correlations illustrated in the right panel. (Right) Correlations as function of the excitation energy between the (n,2n) cross section at 14 MeV and a few other cross sections (see text for details).

A typical illustration is shown in Fig. 18. In this plot, one can for instance observe that the (n,2n) cross section at 14 MeV is correlated with the (n,3n) between 20 and 30 MeV and anti-correlated both with the (n,n') and the (n,2n) in the same interval. This means, as illustrated by the arrows in the left panel of Fig. 18, that if one modify the sampled parameters of the TALYS input to increases the (n,2n), such a change will result in an increase of the (n,3n) above 20 MeV and simultaneously a decrease of the (n,n') and of the (n,2n) in the same energy range.

Total Monte Carlo with TALYS

Another way of using TALYS is the so-called Total Monte Carlo approach. In this case, the sampling is again performed but this time to produce thousands of evaluated nuclear data files [ENDF] and thousands of macroscopic data such as K_{eff}, the effective neutron multiplication factor within an assembly of fissile material such as a nuclear reactor or a macroscopic experiment also called integral experiment. In this case, on top of the cross

sections model uncertainties, one also obtain uncertainties related to integral benchmarks, which provides a link between nuclear reaction models predictive power and the nuclear industry applications. The TALYS code is then not used alone but coupled with other codes in order to systematically (i) transform the results of a TALYS run into an evaluated file and (ii) use this file in a simulation code appropriate to model sets of integral benchmark such as those compiled in the "International handbook of evaluated criticality safety benchmark experiments" [ICSBEP].

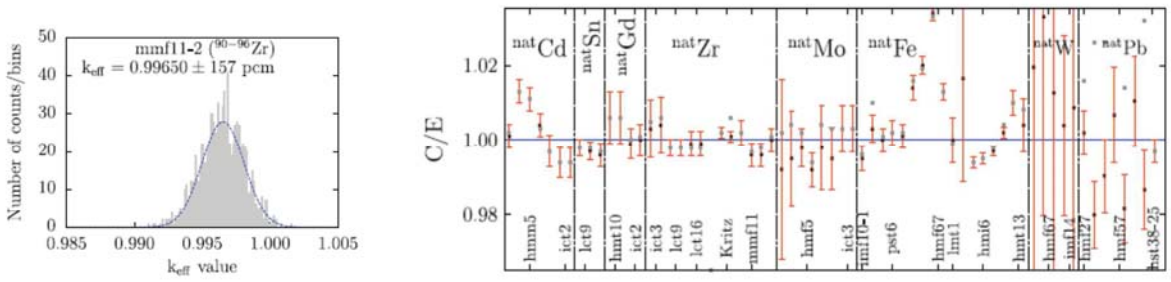

Figure 19: Illustrations of the Total Monte Carlo results. (Left) K_{eff} distribution for a specific benchmark. (Right) Ratio of the Calculated (C) to the Experimental (E) value of several Keff.

In Fig. 19, the results obtained within this framework [Roch2009] are shown for a selected list of benchmarks. In the left panel, one can observe that the distribution of the various calculated K_{eff} looks close to a Gaussian law. In the right panel, is reported the result of 60000 runs for many benchmarks in which on top of the mean K_{eff} values one also shows the standard deviation deduced from the distribution per benchmark as illustrated in the left panel.

e. TENDL : Talys Evaluated Nuclear Data Library

Because of its robustness and of its ability to produce a large part of the data needed in an evaluated file, the TALYS code has been used to produce the so-called "TENDL" library. Its originality comes from the fact that it is a "complete" library produced with a unique methodology with a minimum manual intervention. It is complete in the sense that all information which is relevant to produce an evaluated file is provided including uncertainties and for a number of nuclei which much larger than in any other library. However, for a specific nucleus whose impact is crucial for a nuclear application, the quality of TENDL is not, by default, at the level of the more sophisticated libraries for which a specific fine tuning of parameters has been performed. In general there are 3 categories:

1. At the first extreme, isotopes without any experimental reaction information (about 1600 isotopes). In this case, as no specific information can be used to adjust calculations, we fully rely on systematics, as defined in TALYS or the underlying optical model potential and level density model
2. In between the two extremes, isotopes with scarce experimental data such as thermal cross sections, resonance integrals, average cross sections at high energy (about 400 isotopes). The model parameters are adjusted to reproduce the existing data (such as cross sections or existing resonances).
3. At the other end of the spectrum, isotopes with measured pointwise cross sections, resonances, integral measurements, and resolved resonance parameters (about 400 isotopes). The resonance estimation method can still be applied, but great care should be taken that the modifications do not deteriorate their performances.

As a starting point for resonance estimation, energy dependent statistical parameters as well as specific cross sections are needed in the whole energy range. These parameters are for each orbital angular momentum l and spin of the resonance state j:

- the scattering radius r,
- the average level spacing D0,
- the average reduced neutron width Γ_{0n},
- the average radiation width Γ_{γ},

and if relevant the average fission width Γ_{f}.

The necessary cross sections, consistent with the above parameters are the elastic, capture, inelastic and fission cross sections. These pointwise cross sections can be kept as is above an arbitrary energy limit, usually lower than the first inelastic level. Below this energy limit the average parameters can be converted into statistical resonance structures. This energy limit can be arbitrary chosen, but in practice, it defines the number of resolved resonances and should therefore not be too high.

The quality of the evaluations in the fast neutron range can be classified in three categories, depending on the amount of "knowledge" (e.g. experimental data) which is included in the calculation scheme. For the vast majority of unstable nuclei except the actinides, in the absence of experimental information, default TALYS calculations were performed to obtain cross sections, angular distributions and differential data. These results were directly formatted to the ENDF-6 format. Default model parameters were then applied, which follows systematics globally adjusted for stable isotopes. For stable isotopes, actinides and long-lived nuclei for which experimental data are available, adjusted TALYS parameters were used to reproduce experimental information. In the case of some particularly important isotopes (such as 235U or 238U), an extra step in the evaluation procedure is made, applying minor adjustments to cross sections to obtain good benchmark results.

In the mass range $19 < A < 210$, default and adjusted TALYS calculations were performed. For TENDL, TALYS parameters were adjusted to obtain good agreement between calculated total and partial cross sections and experimental data. For each target nuclide, typically 10-20 TALYS input parameters are adjusted and stored in a database. The most often changed parameters are the real volume radius and diffuseness of the optical model, the particle-hole state density parameters for the pre-equilibrium process, the total level density parameters a of the compound and residual nuclides, and the knockout and stripping parameters to adjust the (n,α) cross sections This has been done for hundreds of nuclides.

6. Conclusion and prospects

The modelling of a nuclear reaction is a complicated task, sometimes challenging. Several models and nuclear ingredients have to be linked together to be able to predict the outcome of a nuclear reaction. Although significant improvements have been made during the last decades, there are still many challenges one has to face. Pre-equilibrium and fission modelling are certainly among these. In the case of pre-equilibrium, the main reason is that the flexibility of semi-classical approaches enables to obtain at small computational price results which satisfy the quality required for applications. It is only recently, that the need for better models has become timely, in particular while studying "subtle" processes such as (n,xnγ) transitions in actinides [Kerv2013]. For fission, the problem is more complicated. The models used are far too simple compared to the most fundamental approaches which need to

account for multidimensional energy landscapes and constraints in order to reach accuracy far below the requirements [Dubr2012]. If the future consists without any doubt in adding more and more microscopic approaches in the nuclear reaction models, this will be a very long term project. For now, such microscopic approaches can only provide guidelines for nuclear data evaluations.

Références :

[Audi2012] G. Audi et al., Chin. Phys. C 36 (2012) 1287.
[Sobi2014] A. Sobiczewski and Y. Litvinov, Phys. Rev. C 90 (2014) 017302.
[Audi2003] G. Audi et al., Chin. Phys. C 36 (2012) 1287.
[EXFOR] *https://www-nds.iaea.org/exfor/4*
[Koni2003] A.J. Koning and J.P. Delaroche, Nucl. Phys. A 713 (2003) 231.
[Mori2004] B. Morillon and P. Romain, Phys. Rev. C 70 (2004) 014601.
[Baug2001] E. Bauge et al., Phys. Rev. C 63 (2001) 024607.
[Dupu2006] M. Dupuis et al., Phys. Rev. C 73 (2006) 014605.
[Koni1998] A.J. Koning and J.M. Akkermans, Workshop on Nuclear reaction Data and Nuclear reactors: Physics, design and safety, ed. P. Oblozinsky and A. Gandini, Feb 23 - March 27 1998, ICTP, Trieste, Italy (1998) 143.
[Hila2007] S. Hilaire and M. Girod, EPJA 33 European Physical Journal A 33 (2007) 237.
[Dela2010] J.P. Delaroche et al., Phys. Rev. C 81 (2010) 014303.
[Dupu2010] M. Dupuis et al., EPJ Web of Conferences, vol. 2, Les Ulis (2010), p. 11001.
[Agas1975] D. Agassi et al., Phys. Rep. 22 (1975) 145.
[Tamu1982] T. Tamura et al., Phys. Rev. C 26 (1982) 379.
[Fesh1980] H. Feshbach et al., Ann. Phys. (NY) 125 (1980) 429.
[Haus1952] W. Hauser and H. Feshbach, Phys. Rev. 87 (1952) 366.
[Kawa2013] T. Kawano, Private communication.
[Hila2003] S. Hilaire et al., Annals of Physics 306 (2003) 209.
[Koni2008] A.J. Koning et al., Nuclear Data for Science and Technology, ed. O. Bersillon et al. (EDP Sciences) 2008 p 211.
[Capo2009] R. Capote et al., Nucl. Data Sheets 110 (2009) 3107.
[Szef1983] Z. Szeflinksi et al., Phys. Lett. B 126 (1983) 159.
[Hill1953] D.L. Hill and J.A. Wheeler, Phys. Rev. 89 (1953) 1102.
[Sin2008] M. Sin and R. Capote, Phys. Rev. C 77 (2008) 054601.
[Igna1975] A.V. Ignatyuk et al., Sov. J. Nucl. Phys. 21 (1975) 255.
[Igna1985] A.V. Ignatyuk, Rep INDC (CCP)-233 International Atomic Energy Agency, Vienna, Austria (1985).
[Gori2008] S. Goriely et al., Phys. Rev. C 78 (2008) 064307.
[Youn1992] P.G. Young et al., LOS ALAMOS report LA-12343-MS, 1992.
[Blan1993] M. Blann, *Workshop on Computation and Analysis of Nuclear Data Relevant to Nuclear Energy and Safety*, edited by M.K. Mehta and J.J. Schmidt, Feb. 10 - March 13 1992, Trieste, Italy (1993) p 622.
[Uhl1976] M. Uhl and B. Strohmaier, IRK report No. 76/01, Vienna (1976).
[Herm2007] M. Hermann et al., Nucl. Data Sheets 108 (2007) 2655.
[Rayn1994] J. Raynal, CEA Saclay Report No. CEA-N-2772, (1994).
[ENDF] ENDF-102 data format and procedures for the evaluated data file ENDF-6, rapport BNL-NCS-44945-01/04Rev, Brookhaven USA.
[Goko2006] S. Goko et al.,Phys. Rev. Lett. 96 (2006) 192501.
[TALYS] http://www.talys.eu
[ICSBEP] International handbook of evaluated criticality safety benchmark experiments, NEA/NSCDOC(95)03, NEA Paris 2005.

[Roch2009] D. Rochman et al., Ann. Nuc. En. 36 (2006) 810.
[Kerv2013] M. Kerveno et al., Phys. Rev. C 87 (2013) 024609.
[Dubr2012] N. Dubray et al., Comp. Phys. Comm. 183 (2012) 2035.